Cancer Cell, Volume *30*

Supplemental Information

Critical Role for CD103^{+}/CD141^{+} Dendritic Cells Bearing CCR7 for Tumor Antigen Trafficking and Priming of T Cell Immunity in Melanoma

Edward W. Roberts, Miranda L. Broz, Mikhail Binnewies, Mark B. Headley, Amanda E. Nelson, Denise M. Wolf, Tsuneyasu Kaisho, Dusan Bogunovic, Nina Bhardwaj, and Matthew F. Krummel

Supplemental Data

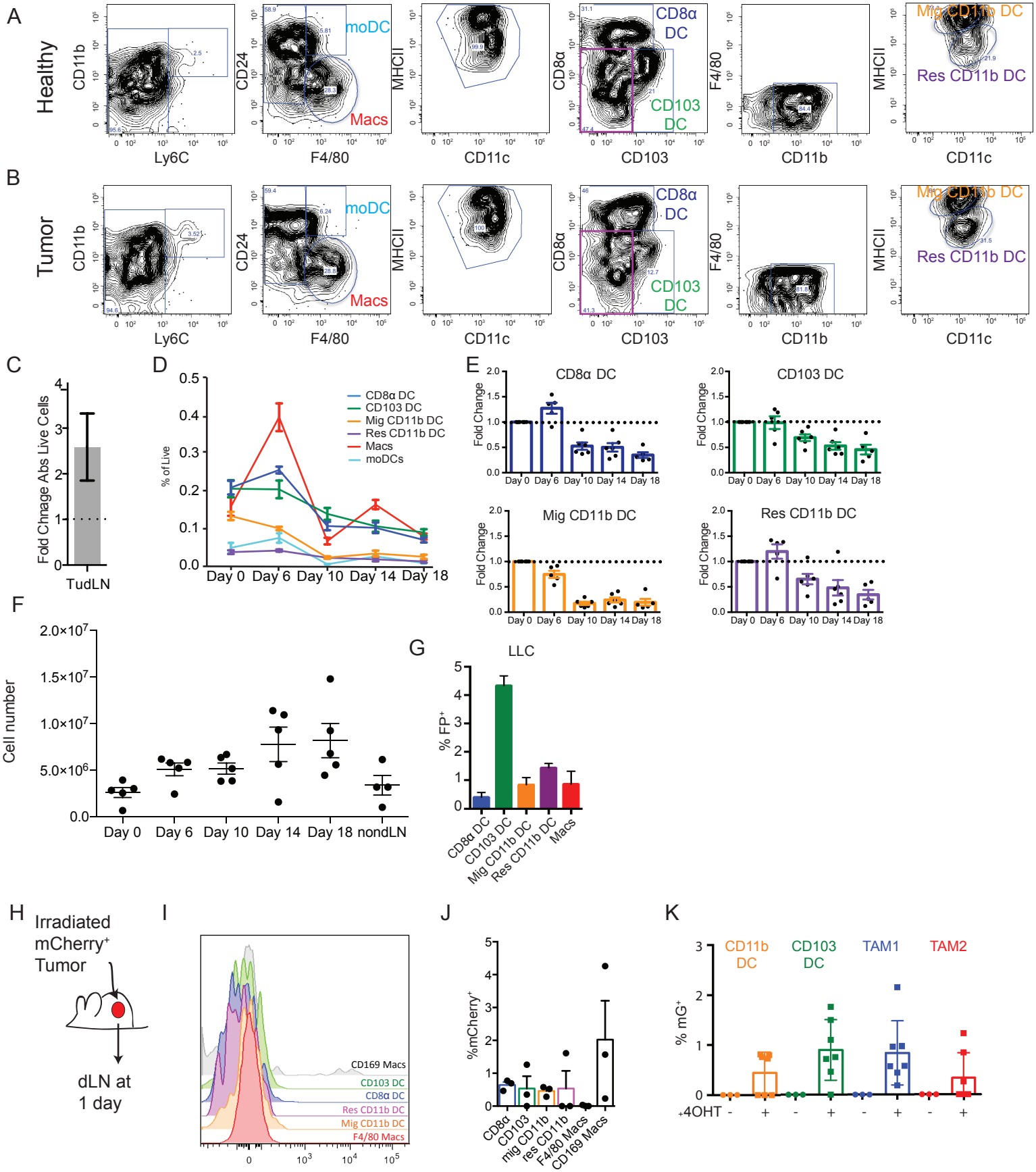

Figure S1. Related to Figure 1. Progression and dissection of the tumor draining lymph node environment

(A) Gating strategy for the delineation of the healthy LN myeloid compartment. Combined inguinal and axillary LN. Progressive gating identifies LN Macrophages, $CD8\alpha^+$ DC, migratory $CD103^+$ DC, and resident and migratory $CD11b^+$ DC subsets. Data shown are representative of greater than 3 experiments.

(B) Gating strategy for the delineation of the B78ChOVA melanoma tumor dLN myeloid compartment. Combined inguinal and axillary LN. Progressive gating identifies LN macrophages, $CD8\alpha^+$ DC, migratory $CD103^+$ DC, and resident and migratory $CD11b^+$ DC subsets. Data shown are representative of greater than 5 experiments.

(C) Fold change in total live cells in tumor dLN (inguinal and axillary) from day 18 B78ChOVA tumor-bearing mice (n=3) compared to healthy inguinal and axillary LN as measured by flow cytometry. Data were pooled from 2 independent experiments and plotted as mean ±SEM from individual LN (n=3).

(D) Proportional changes among the myeloid tumor dLN populations (as defined by the gating in Fig. 1A, B for inguinal and axillary LN) with B78ChOVA melanoma tumor progression. Data were plotted as mean ± S.E.M. for each population as a percentage of total live cells (n=3).

(E) Fold change in percent of live LN cells relative to healthy LN DC populations for $CD8\alpha^+$ DC, $CD103^+$ DC, migratory $CD11b^+$ DC and resident $CD11b^+$ DC over the progression of tumor growth. Dotted line represents relative populations in healthy LNs. Plotted as mean fold change ±SEM for each population (n=3).

(F) Quantified cell number from the dLN over the progression of tumor growth (n=5). Data were plotted as mean ± S.E.M.

(G) Frequency of tumor $antigen^+$ DC populations across the tumor dLNs of multiple LLC tumors. Data were plotted as mean ± S.E.M. for each population.

(H) Schematic of assessment for LN drainage of mCherry after s.c. inoculation with irradiated cells.

(I) Representative histogram of tumor-derived mCherry fluorescence across the tumor dLN populations of the inguinal and axillary LN 24 hours after subcutaneous injection of lethally irradiated B78ChOVA tumor cells.

(J) Frequency of $mCherry^+$ DC populations across the tumor dLNs of multiple mice injected s.c. with irradiated B78ChOVA cells (n=3). Data were plotted as mean + S.E.M.

(K) Histograms showing marking of tumor myeloid populations 24 hours after 3 daily intratumoral injections of 4OHT ($n \geq 4$ for all groups). Plotted as mean ± S.E.M. Data are representative of 5 independent experiments.

Movie S1. Related to Figure 2. XCR1^{+} mCherry^{+} DC interact with OTI cells in the tumor dLN in vivo.
Multiphoton live-imaging of tumor-draining LNs of B78ChOVA-bearing *XCR1*-Venus mice 2 days after transfer of 2x10^{6} GFP^{+} OTI T cells. OTI T cells are labeled green, XCR1^{+} cells in yellow and mCherry in red. Scale Bar indicated. Frame rate: 9.4FPS.

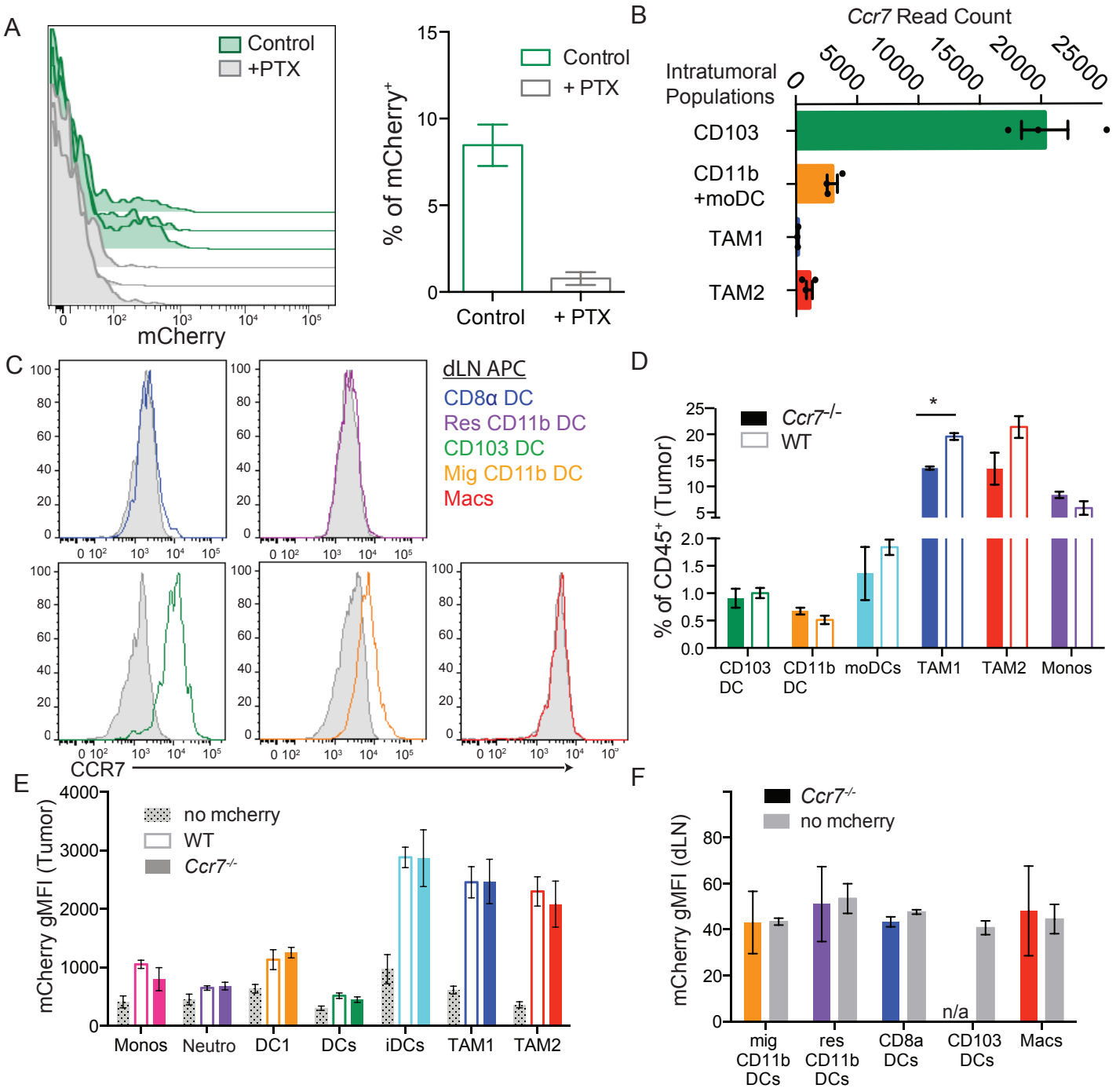

Figure S2. Related to Figure 3. Prevention of CCR7 dependent migration to the dLN reduces tumor antigen accumulation in all myeloid compartments of the tumor dLN.

(A) Representative flow cytometric histogram and quantification of tumor-derived mCherry fluorescence in the CD103$^+$ DC in the tumor dLNs of animals either treated with 0.5 ug of PTX (grey) or PBS (green) for 5 days (n=3). Data were pooled from dual flank-bearing tumor animals, and plotted as mean ± S.E.M. for each population (n=3) and are representative of 3 independent experiments.

(B) Mean transcript read counts for *Ccr7* expression in tumor-derived CD103$^+$ DC (green), CD11b$^+$ DC (orange), TAM1 (blue), and TAM2 (red) populations in primary melanoma tumor tissue, as quantified by RNASeq analysis. Data were plotted as mean ± S.E.M. for each population over three biological triplicates (n=3).

(C) Representative flow cytometric histograms of CCR7 levels on tumor dLN myeloid populations (colored) compared to isotype control (grey) (n=3).

(D) Representative histogram quantifying the proportion of the CD45$^+$ compartment composed of each tumor myeloid population in *Ccr7*$^{-/-}$ and age and sex matched WT controls (n=5). Data were plotted as mean ± S.E.M. * = $p<0.05$

(E) Quantification of tumor-derived mCherry fluorescence within the myeloid populations in the primary tumors of *Ccr7*$^{-/-}$ tumor-bearing mice. Data were plotted as mean ± S.E.M.

(F) Quantification of tumor-derived mCherry fluorescence within the myeloid populations in the tumor-draining LN of *Ccr7*$^{-/-}$ tumor-bearing mice. Data were plotted as mean ± S.E.M.

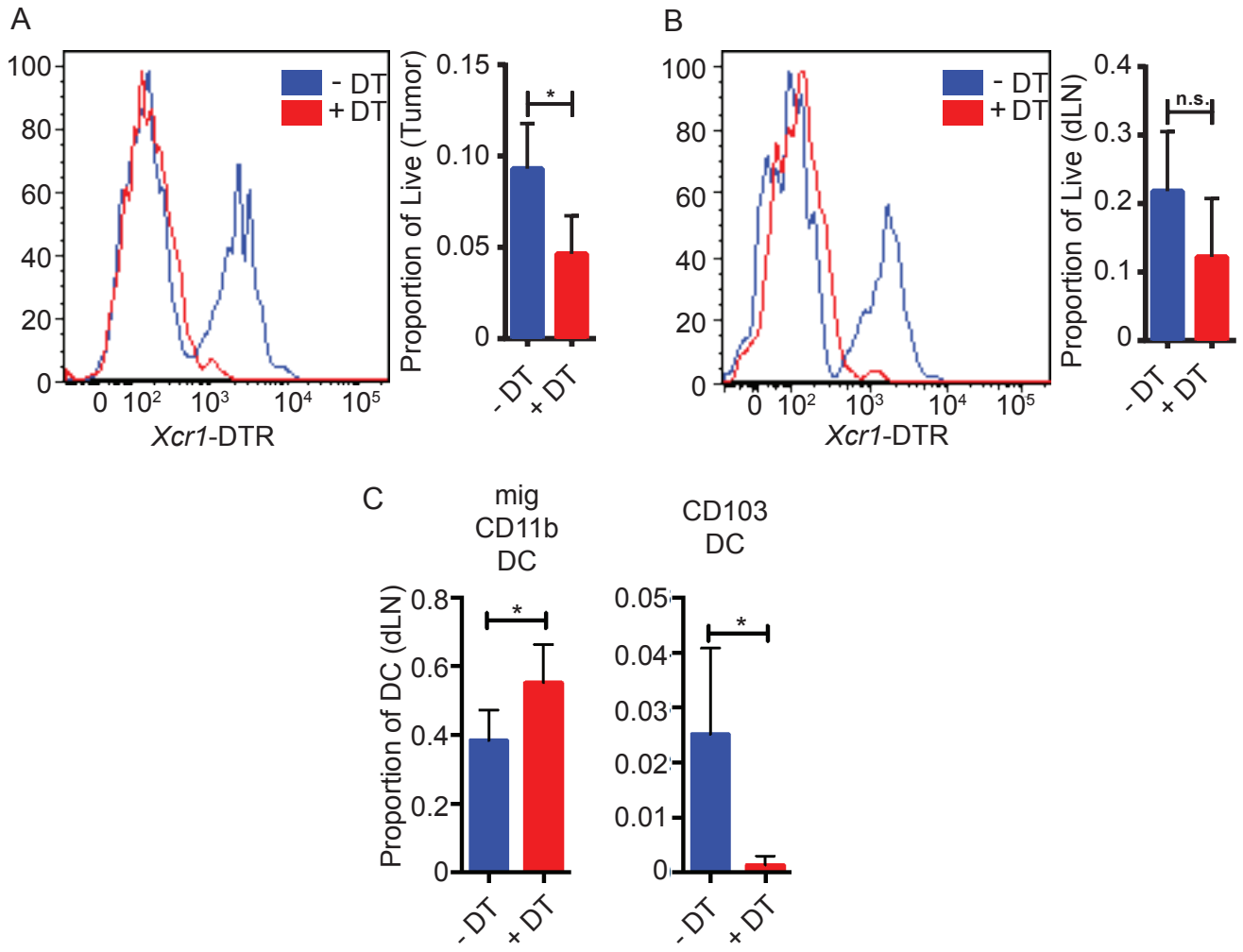

Figure S3. Related to Figure 5. DT administration to mixed *Ccr7*$^{-/-}$:*XCR1*-DTR BM chimeras selectively depletes dLN CD103^{+} DC.

(A) Representative flow cytometric histogram showing XCR1-DTR levels in intratumoral CD103^{+} DC in *XCR1*-DTR:*Ccr7*$^{-/-}$ mixed BM chimera animals either treated every three days with 0.5 mg of diphtheria toxin (red) or PBS (blue). Data were plotted as mean ± S.E.M. for each population over three biological triplicates (n=3). * = $p<0.05$.

(B) Representative flow cytometric histogram showing XCR1-DTR levels in dLN CD8α^{+} DC in *XCR1*-DTR:*Ccr7*$^{-/-}$ mixed BM chimera animals either treated every three days with 0.5 mg of DT (red) or PBS (blue). Data were plotted as mean ± S.E.M. for each population over three biological triplicates (n=3).

(C) Quantification of proportion of dLN DC that are either migratory CD11b^{+} or CD103^{+} in *XCR1*-DTR:*Ccr7*$^{-/-}$ mixed BM chimera animals either treated every three days with 0.5 mg of DT (red) or PBS (blue). Data were plotted as mean ± S.E.M. for each population over three biological triplicates (n=3). * = $p<0.05$.

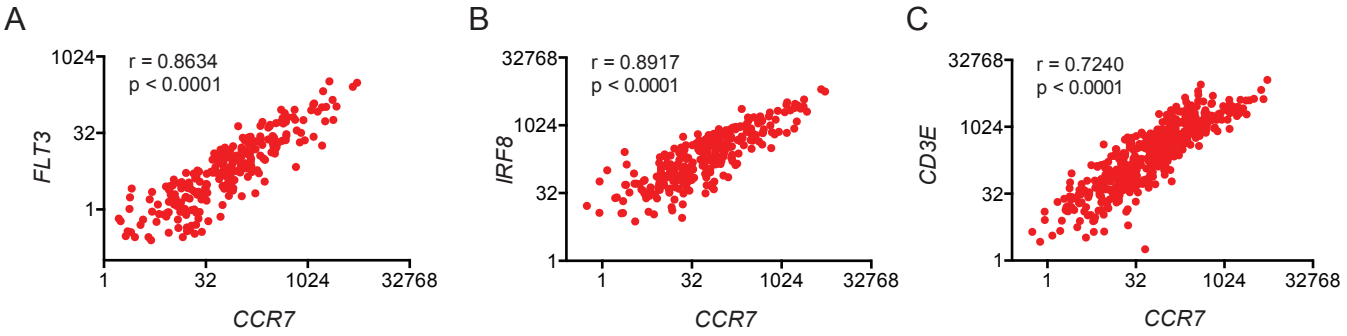

Figure S4. Related to Figure 6. ***CCR7*** **levels in human tumors correlate with markers of migratory CD141^{+} DC.**
(A) Scatter plot showing correlation of *FLT3* and *CCR7* transcript levels, determined by RNASeq, in melanoma samples. Data from the skin cutaneous melanoma provisional TCGA dataset, n=471. Pearson correlation coefficient is shown.
(B) Scatter plot showing correlation of *IRF8* and *CCR7* transcript levels, determined by RNASeq, in melanoma samples. Data from the skin cutaneous melanoma provisional TCGA dataset, n=471. Pearson correlation coefficient is shown.
(C) Scatter plot showing correlation of *CD3E* and *CCR7* transcript levels, determined by RNASeq, in melanoma samples. Data from the skin cutaneous melanoma provisional TCGA dataset, n=471. Pearson correlation coefficient is shown.

Supplemental Experimental Procedures

Cell lines and ectopic tumor injection

B78ChOVA, B78 parental cells transfected with a ChOVA fusion construct identical to that used in PyMTChOVA (Engelhardt et al., 2012) were harvested and washed 3 times with PBS, mixed at a 1:1 ratio with growth factor-reduced Matrigel Matrix (BD Biosciences) in a final injection volume of 50 μl. $1.5x10^5$ (unless otherwise stated) were injected subcutaneously in the right and left flanks of shaved mice and allowed to grow for 14-21 days before use. Briefly, adherent cells were cultured at 37°C with 5 % CO2 in DMEM plus 10 % FCS with Penicillin, Streptomycin and Glutamine on tissue culture-treated plastic plates and split every other day.

Bone Marrow chimera generation

To generate BM chimeras WT mice were lethally irradiated by exposure to 1,100 rads of γ-irradiation in 2 doses, 3 hours apart. 2-5 $x10^6$ BM cells, consisting of 50% *Ccr7*$^{-/-}$ or WT BM and 50% *Xcr1*-DTR BM, were injected retro-orbitally to reconstitute irradiated mice. Chimeric mice were analyzed 8-10 weeks after reconstitution.

Cell isolation

Naive OTI T cells were isolated from LNs and spleen of 6- to 12-week-old mice. Selection was carried out with a negative CD8 isolation kit (Stemcell Technologies) following manufacturer's instructions. BMDCs were generated by culture of bone marrow cells for 8–11 days plated at 1-$2x10^6$ cells/ml in IMDM (Iscove's Modified Dulbecco's Medium) with 10 % FCS (HyClone) with GM-CSF (granulocyte-macrophage colony-stimulating factor). 75 U/ml IL-4 was added for the final 2 days of culture and 10 μg LPS (E. coli derived, Sigma) was added 12 hours before use to fully mature the BMDC.

In vivo labeling of tumor resident cells

$1.5x10^5$ B16F10 cells were injected subcutaneously on the flank of *Ubc-CreERT2* mTmG mice and at day 10, 11 and 12 of tumor growth 20 μl of 4OHT (Sigma) in DMSO was injected intra-tumorally. On day 13 tumor dLNs were harvested, digested and analyzed by flow cytometry.

Adoptive T cell transfers

OTI$^+$ CD45.1$^+$ T cells were harvested from the LNs of OTI transgenic mice, and CD8 negatively selected with a magnetic bead enrichment (EasySep) and labeled with 5 μM of VPD450. Labeled T cells were washed 3 times in PBS and injected i.v. at 1-$5x10^5$ cells per mouse. After 2 days, recipient tumor-bearing mice were harvested for analysis of transferred T cells in tumor-draining LNs.

PTX Treatment

Tumor-bearing mice were injected i.p. daily for 5 consecutive days with 0.5 μg of PTX in PBS.

Confocal Imaging

DC populations were sorted (based on the gating strategy in Fig. 1A) using a FACS Aria II flow cytometer from tumor-draining LNs and plated onto coated glass slide chambers and then imaged on a confocal Nikon A1R microscope.

Two Photon Microscopy

Intravital imaging was performed using a custom-built two-photon setup equipped with two infrared lasers (MaiTai: Spectra Physics, Chameleon: Coherent). The MaiTai laser was tuned to 810 nm for excitation of CFP. Chameleon laser excitation was tuned to 980 nm for simultaneous excitation of Venus, mCherry and GFP. Emitted light was detected using a 25x 1.2 NA water lens (Zeiss) coupled to a 6-color detector array (custom; utilizing Hamamatsu H9433MOD detectors). Emission filters used were: blue 475/23, green 510/42, yellow 542/27, red 607/70, far red 675/67. The microscope was controlled by the MicroManager software suite, z-stack images were acquired with 4-fold averaging and z-depths of 3 μm. Data analysis was performed using the Imaris software suite (Bitplane). To characterize contact parameters between T cells and DCs, tracks and surface of T cells and DCs were generated, and the dwell time of interaction between surfaces was analyzed as previously described (Gerard et al., 2014): T cell–DC cell interaction was defined as the association at 4 μm or less of a given OTI cell surface with a DC surface, with an initial threshold of this contact of at least 1 min.

LN Explant imaging

Imaging was performed as previously described(Gerard et al., 2014). $2x10^6$ GFP expressing OTI Cells were transferred in B78ChOVA bearing *Xcr1*-Venus mice 2 days prior to imaging. Inguinal and axillary lymph nodes was removed, cleaned of fat, and immobilized on a plastic coverslip with the hilum facing away from the objective. LN were imaged in 30 minute intervals with 810 nm excitation on a two-photon microscope as per above.

Statistical Analysis

Statistical analyses were performed using GraphPad Prism software. Unless specifically noted, all data are representative of >3 separate experiments. Error bars represent standard error of the mean (S.E.M.) calculated using Prism, and are derived from triplicate experimental conditions. Specific statistical tests used were paired and unpaired T tests and p values <0.05 were considered statistically significant.

Supplemental References

Gerard, A., Patino-Lopez, G., Beemiller, P., Nambiar, R., Ben-Aissa, K., Liu, Y., Totah, F. J., Tyska, M. J., Shaw, S., and Krummel, M. F. (2014). Detection of Rare Antigen-Presenting Cells through T Cell-Intrinsic Meandering Motility, Mediated by Myo1g. Cell 158, 492-505.